Dental Materials Journal 2015; 34(3): 302–309

Improving shear bond strength between feldspathic porcelain and zirconia substructure with lithium disilicate glass-ceramic liner

Kamolporn WATTANASIRMKIT[1], Viritpon SRIMANEEPONG[1], Kanchana KANCHANATAWEWAT[2], Naruporn MONMATURAPOJ[3], Pasutha THUNYAKITPISAL[4] and Supatra JINAWATH[5]

[1] *Department of Prosthodontics, Faculty of Dentistry, Chulalongkorn University, Pathumwan, Bangkok 10330, Thailand*
[2] *Institute of Advanced Dental Medicine, Rangsit University, Bangkok, Thailand*
[3] *National Metal and Materials Technology Center (MTEC), Pathumthani, Thailand*
[4] *Research Unit of Herbal Medicine and Natural Product for Dental Treatment, Department of Anatomy, Faculty of Dentistry, Chulalongkorn University, Pathumwan, Bangkok 10330, Thailand*
[5] *Department of Materials Science, Faculty of Science, Chulalongkorn University, Pathumwan, Bangkok 10330, Thailand*
Corresponding author, Viritpon SRIMANEEPONG; E-mail: viritpon.s@chula.ac.th

This study investigated the shear bond strength (SBS) between veneering porcelain and zirconia substructure using lithium disilicate glass-ceramic as a liner. The mineral phases and microstructures of lithium disilicate glass-ceramic at temperature range of 800–900°C were preliminarily investigated. SBSs of porcelain-veneered zirconia specimens with and without lithium disilicate glass-ceramic liner fired at the same temperature were determined. Results showed that SBSs of veneering porcelain and zirconia with lithium disilicate glass-ceramic liner was notably increased ($p<0.05$). Specimens from the group with the highest SBS (59.7 MPa) were subject to thermocycling up to 10,000 cycles and their post-thermocycling SBSs investigated. Though weakened by thermocycling, SBSs were above the clinically acceptable limit (25 MPa) of ISO 9693. Fractographic analysis revealed mixed cohesive and adhesive failures. It was concluded that lithium disilicate glass-ceramic is a potential liner which generated high SBS between veneering porcelain and zirconia.

Keywords: Zirconia, Feldspathic porcelain, Shear bond strength, Thermocycling

INTRODUCTION

An all-ceramic dental restoration composed of porcelain veneer on a zirconia substructure has become a popular alternative to metal-ceramic restorations due to its comparatively high mechanical strength. Although zirconia restorations seem to meet both esthetic and mechanical demands, chipping or delamination of the porcelain veneer is a frequently reported problem[1-3]. Veneering porcelain is prone to chipping due to brittleness. Chipping aggravated by residual stress may cause delamination of veneering porcelain from the zirconia substructure. Mechanical methods —such as sandblasting, grinding and glass joining— have emerged in a bid to improve the bond strength between zirconia substructures and veneering porcelains[4-6].

Glass joining, being used for industrial applications such as decorative stained glass or fuel cell technology, is also used for the fabrication of dental prostheses by producing a glass or glass-ceramic interlayer between veneering porcelain and zirconia substructure[6]. Currently, the commercially available glass-ceramic interlayer is either feldspathic porcelain or a mixture of feldspathic porcelain and leucite crystals. The interlayer is a liquid suspension between zirconia substructure and veneering porcelain used to enhance their adhesion.

The coefficient of thermal expansion (CTE) of feldspathic porcelain at 25–500°C is about 8.8–9.2×10^{-6} K^{-1}. Feldspathic porcelain tends to form additional leucite[7] ($KAlSi_2O_6$; CTE (25–700°C): ~20–25×10^{-6} K^{-1})[8,9] during firing, which consequently reinforces the mixture. Multiple firing cycles also trigger the formation of additional leucite due to the reaction between the constituent ions of feldspathic porcelain. This may then affect the CTE value of the veneering feldspathic porcelain in consideration of the large CTE value of leucite[10,11]. Dissimilarities in CTE values between two materials bonded together will impair a stable long-term bond between the two materials.

Lithium disilicate (CTE (25–800°C): ~9.3–9.9×10^{-6} K^{-1}) is another type of glass ceramic which offers thermal shock resistance, thus leading to a more stable CTE after multiple firing[12]. Moreover, lithium disilicate has CTE close to that of the veneering feldspathic porcelain and zirconia substructure.

The purpose of the present study was to investigate the possibility of using lithium disilicate glass-ceramic as a liner between veneering feldspathic porcelain and zirconia substructure. Shear bond strength and thermocycling were used to characterize the performance of the lithium disilicate glass-ceramic liner. Null-hypotheses tested in this study were: (1) Lithium disilicate glass-ceramic would have no effect on shear bond strength between zirconia and veneering porcelain; and (2) Thermocycling treatment would have no effect on shear bond strength between zirconia and veneering porcelain using lithium disilicate glass-ceramic as a liner.

Color figures can be viewed in the online issue, which is available at J-STAGE.

Received Nov 20, 2014: Accepted Dec 16, 2014
doi:10.4012/dmj.2014-319 JOI JST.JSTAGE/dmj/2014-319

MATERIALS AND METHODS

Details of the materials used in this study are shown in Table 1.

Preparation of lithium disilicate glass-ceramic pellets
Lithium disilicate glass-ceramic liner was obtained from the National Metal and Materials Technology Center, Pathumthani, Thailand[13]. Specimens were divided into three groups (n=8) according to three different firing temperatures: 800°C (Li 800), 850°C (Li 850), and 900°C (Li 900). Glass-ceramic liner pellets, 3 mm in diameter and 2 mm in thickness, were fabricated from lithium disilicate powder mixed with VITA VM® 9 Effect Bonder Fluid (VITA Zahnfabrik, Bad Säckingen, Germany). Mixture was pressed in an acrylic mold and vibrated to condense the solid, and the liquid was drained out.

1. X-ray diffraction (XRD) analysis of mineral phases
The mineral phases of glass-ceramic liner pellets were investigated using an X-ray diffractometer (Bruker D8, Bruker AXS, Karlsruhe, Germany), operated between 5° and 80° 2θ, with a step width of 0.01° 2θ. After firing, the mineral phases were identified by comparing the obtained diffraction patterns with the diffraction standards of International Center for Diffraction Data (ICCD or JCPDS).

2. Scanning electron microscopy (SEM) analysis of microstructure
After being fired at their respective temperatures, the pellets were polished with #600, #800, and #1,000 silicon carbide papers and finished with 9-, 6-, 3-, and 1-μm diamond paste (Leco, LECO Corp., Michigan, USA). After for 5 min of cleaning in distilled water using an ultrasonic cleaner, the pellets were coated with gold particles by an ion beam sputtering device for microstructure observation by SEM (JSM-6400 Scanning Electron Microscope, JEOL Ltd., Tokyo, Japan).

Preparation of porcelain-veneered zirconia specimens
Thirty-two square specimens (10 mm×10 mm×2 mm) of pre-sintered zirconia (VITA In-Ceram® YZ, VITA Zahnfabrik, Bad Säckingen, Germany) were prepared from the commercial blocks using an IsoMet cutting machine (Buehler, Lake Bluff, IL, USA). The specimens were fully sintered in a furnace according to manufacturer's recommendation to achieve a density of 99% of theoretical density.

A piece of 0.1-mm-thick clear plastic tape with a 3-mm-diameter hole in the center was applied to 24 fully sintered zirconia specimens (about 30% shrinkage). This was done to define the bonding area and thickness of the coating layer according to ISO Technical Specification ISO/TS 11405:2003[14]. A layer of lithium disilicate glass-ceramic paste (lithium disilicate glass-ceramic powder mixed with VITA VM® 9 Effect Bonder Fluid) was applied to the surfaces of all sintered zirconia specimens. After the tape was removed from the zirconia surface, the specimens were divided into three groups with eight specimens per group. Specimens in each group were fired at the respective temperature of 800°C (VITALi800 group), 850°C (VITALi850 group), or 900°C (VITALi900 group) in VITA VACUMAT 4000T furnace (VITA Zahnfabrik, Bad Säckingen, Germany).

Eight specimens of sintered zirconia without liner (VITAD) were prepared to serve as the control group. A specimen each from the control group and the above-mentioned three groups with lithium disilicate glass-ceramic liner were secured in a split acrylic mold of 3 mm diameter and 1 mm height. Three layers of veneering porcelain (dentin) paste were incrementally applied

Table 1 Details of the materials used in this study (publicly available on the manufacturers' website)

Materials		Manufacturer	Batch No.	Main Composition [wt%]	CTE. [$10^{-6}K^{-1}$]
Zirconia substructure	VITA In-Ceram® YZ for inLab®	VITA Zahnfabrik, Germany	10730	ZrO_2 95 wt%, Y_2O_3 5 wt%, HfO_2<3 wt%, Al_2O_3 and SiO_2 & other oxides<1 wt%	10.5
Lining material	lithium disilicate glass-ceramic (test-group)	National Metal and Materials Technology Center, Thailand (MTEC)	—	SiO_2 60 wt%, LiO_2 30 wt%[13]	9.3
Veneering Porcelain	VITA VM® 9 Base dentin	VITA Zahnfabrik, Germany	20470	SiO_2 60–64 wt%, Al_2O_3 13–15 wt%, K_2O 7–10 wt%, Na_2O 4–6 wt%, B_2O 3.3–5 wt%	9±0.2
	VITA VM® 9 Transparent Dentin	VITA Zahnfabrik, Germany	16340	SiO_2 60–64 wt%, $Al_2O_3$13–15 wt%, K_2O 7–10 wt%, Na_2O 4–6 wt%, B_2O 3.3–5 wt%	9±0.2
Liquid	VITA VM® 9 Effect Bonder Fluid	VITA Zahnfabrik, Germany	23550	Ethanol (F. R11) 2.5–10% Sodium hydroxide (C. R35)<2.5%	—

onto all zirconia specimens, following the recommended multiple firing schedule of the manufacturer. The first layer of dentin paste was applied with a brush to fill the mold and fired. The second and third layers of dentin paste were incrementally applied to fill the mold after the first and second firings to compensate the shrinkage. Final thickness of the veneering porcelain was approximately 1 mm. This procedure is illustrated in Fig. 1.

1. Shear bond strength test

Prepared specimens were each embedded in polyvinyl chloride (PVC) rings using polymethyl methacrylate (PMMA) resin and stored in distilled water at 37°C for 24 h before testing. Each specimen was secured in a metal holder and attached to a universal testing machine (Shimadzu, Kyoto, Japan). Each specimen was stabilized to ensure that the edge of the shearing jig touched the zirconia surface and was positioned as close as possible to the veneer-substructure interface following ISO 11405[14]. A shear load was applied at a crosshead speed of 0.5 mm/min. The ultimate load at failure was recorded, and average shear bond strength (MPa) was calculated by dividing the load (N) at which failure occurred by the bonding area (mm^2). Mean shear bond strength and the standard deviation for each group were calculated from these data.

2. Failure analysis

After failure occurred, the specimens were visually analyzed under a stereo microscope (ML9300, Meiji Techno Co. Ltd., Saitama, Japan) at ×1.5 magnification. Failure modes were classified into three types: (1) Cohesive failure within veneering porcelain; (2) Adhesive failure between glass-ceramic liner and zirconia substructure; (3) Combined failure with both cohesive and adhesive failures present.

Specimens were randomly chosen from each group and gold-coated using a sputtering device (Emitech K550 Sputter Coater, Emitech Ltd., Kent, England). For fractographic analysis, these specimens were observed under a scanning electron microscope (JSM-6400 Scanning Electron Microscope, JEOL Ltd., Tokyo, Japan) in back-scatter mode at 15 kV and ×35 magnification. Contrast between the white color of zirconia substructure and the gray color of glass-ceramic liner or veneering porcelain remaining on the zirconia surface were used to determine the failure mode.

Thermocycling test

Specimens of the group that yielded the highest shear bond strength were subject to the thermocycling test. Eight specimens were placed in a water bath (Inmotiontechnology, Bangkok, Thailand) to be thermocycled for 5,000 or 10,000 cycles between 5±2°C and 55±2°C for 125 h (5,000-cycle group) or 250 h (10,000-cycle group). During thermocycling, the dwell time for the specimens in each well was 30 s. Transfer time between the wells was 30 s.

After thermocycling, specimens were embedded in PVC rings using PMMA resin as previously described. They were stored in distilled water at 37°C for 24 h before testing. The SBS test of specimens after thermocycling was performed as described above.

Results of SBS test were analyzed using one-way ANOVA. Fractographic analysis was performed using a stereo microscope and in back-scatter mode of SEM. Mineral phases of the specimens after thermocycling test were investigated for phase transformation, in comparison with the corresponding specimens, by XRD.

Statistical analysis

SPSS statistical analysis software (SPSS Statistics ver. 17, Cary, USA) was used to analyze the data. One-way ANOVA followed by Tukey's HSD test was used for statistical analyses. Significance level was set at

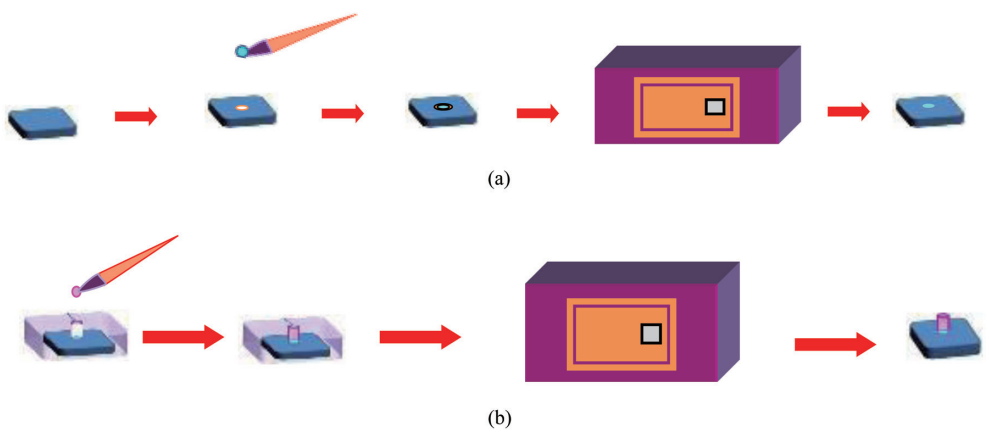

Fig. 1 Preparation of specimens for SBS testing.
(a) A layer of glass-ceramic liner is applied on zirconia surface; (b) Acrylic mold is secured on zirconia surface to act as a template and thickness controller for applying veneering porcelain (dentin) layer.

α=0.05.

RESULTS

Mineral phase and microstructure of fired lithium disilicate glass-ceramic

XRD results in Fig. 2 showed that, regardless of firing temperature, lithium disilicate glass-ceramic liner specimens contained α-quartz (SiO_2), lithium disilicate ($Li_2Si_2O_5$), lithium orthophosphate (Li_3PO_4), and lithium aluminum silicate ($LiAlSi_2O_6$). XRD data also revealed that the prominent phase of lithium disilicate glass-ceramic liner was quartz, followed by $Li_2Si_2O_5$ and Li_3PO_4. Moreover, there were respectively higher amounts of Li_3PO_4 and $Li_2Si_2O_5$ in VITALi 800 and 850 groups, as shown by the higher XRD peaks, compared to VITALi900.

The appearance of lithium disilicate glass-ceramic liner (Li800) revealed small needle-like crystals of $Li_2Si_2O_5$ distributed in a glassy matrix of the original glass-ceramic particles (Fig. 3a). The microstructure of Li850 showed a continuous glass matrix with many large pores in close proximity (Fig. 3b) —which indicated a higher degree of melting, and the presence of long needle-like $Li_2Si_2O_5$ crystals. After firing lithium disilicate glass-ceramic at 900°C, a more homogeneous glassy matrix was observed. There was almost no porosity and the crystals were longer and thinner compared to the other conditions (Fig. 3c).

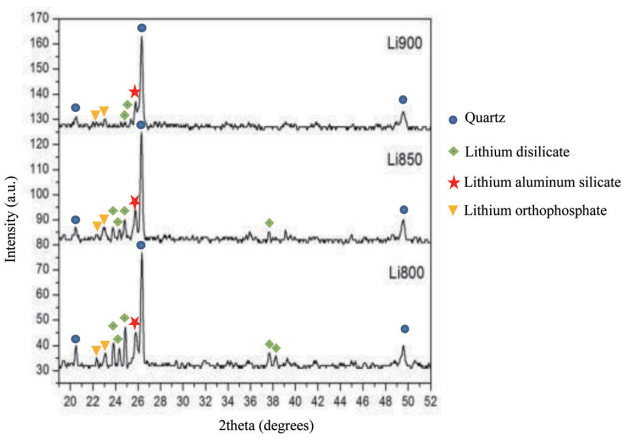

Fig. 2 X-ray diffraction patterns of lithium disilicate glass-ceramic liner specimens fired at temperatures of 800, 850 and 900°C.

Shear bond strength and failure mode

Table 2 shows the SBS results. VITALi850 group demonstrated the highest SBS (59.7 MPa), which was significantly different from the other groups ($p<0.01$). In contrast, VITALi900 group showed the lowest SBS. The mean SBSs of all groups were above the clinically acceptable limit of 25 MPa.

Figure 4 shows the fracture surfaces of VITAD (Figs. 4(a)–(c)) and VITALi850 (Figs. 4(d)–(f)). The control group VITAD demonstrated adhesive failure predominantly. The other three groups with lithium disilicate glass-ceramic liner demonstrated both adhesive and cohesive failures regardless of firing temperature. Cohesive failure is demonstrated by the traces of glass-ceramic liner (lighter areas in the figures) remaining on both the zirconia (Fig. 4e) and feldspathic ceramic surfaces (Fig. 4d). Adhesive failure is demonstrated in the control samples by a clean veneering porcelain surface (Fig. 4a) and zirconia surface (Fig. 4b). This is confirmed by the back-scattered SEM images of the zirconia side of VITAD (Fig.4c) and VITALi850 (Fig. 4f).

Shear bond strength test after thermocycling

All specimens survived after being thermocycled for 5,000 and 10,000 cycles; their mean SBSs were 39.6 MPa and 37.0 MPa respectively. The mean SBS of the control group was 59.7 MPa, which was significantly higher than the thermocycled specimens ($p<0.05$) (Table 3).

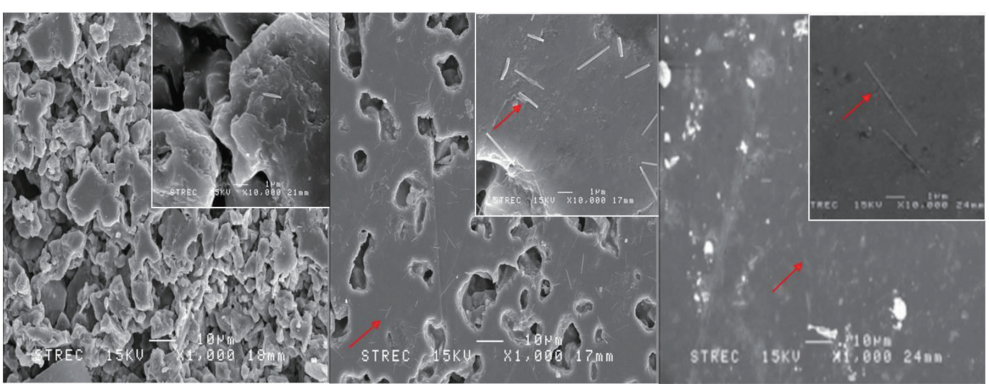

(a) (b) (c)

Fig. 3 Lithium disilicate glass-ceramic liner fired at 800°C (a), 850°C (b) and 900°C (c). Image is shown at ×10,000 magnification at the upper right corner. Red arrows indicate the presence of $Li_2Si_2O_5$ crystals.

Phase transformation after thermocycling
Before thermocycling, the microstructure of VITALi850 specimens was tetragonal. After thermocycling, representative XRD results of VITALi850 in Fig. 5 showed that the microstructure of zirconia surface was partially transformed from tetragonal phase to monoclinic phase regardless of the number of thermocycles.

Microstructural changes after thermocycling
Back-scattered SEM images (Fig. 6) revealed traces of

Table 2 Mean shear bond strengths of porcelain-veneered VITA zirconia substructures with and without lithium disilicate glass-ceramic liners

Group	Shear bond strength (SD) (MPa.)	Mode of failure Ψ		
		Cohesive	Adhesive	Combined
VITAD	41.3 (10.8)	—	5	3
VITALi800D	44.4 (9.2)	—	—	8
VITALi850D	59.7 (4.3) *	2	1	5
VITALi900D	31.0 (10.6) **	—	—	8

(*, ** indicates statistically significant difference from the control at $p<0.01$, Ψ indicates number of specimens)

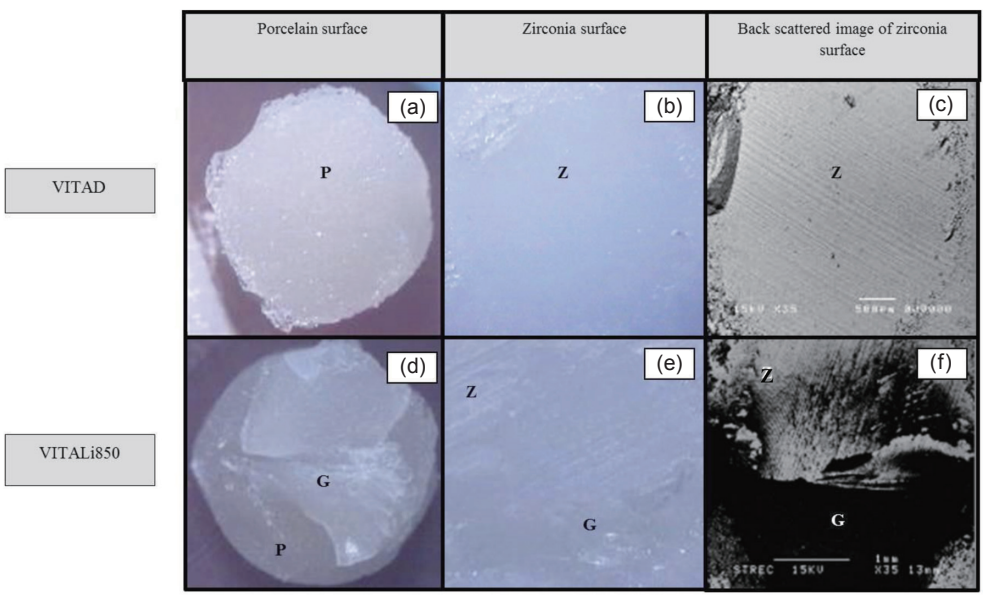

Fig. 4 Stereomicroscopic and back-scattered SEM images of the fracture surfaces.
P in (a) and (d) indicates the exposed veneering porcelain surface; Z in (b), (c), (e) and (f) indicates the exposed zirconia surface; G in (e), (d) and (f) indicates the exposed glass-ceramic surface.

Table 3 Shear bond strength after thermocycling for 0 cycle, 5,000 cycles and 10,000 cycles

Group	Shear bond strength (SD) (MPa.)	Mode of failure Ψ		
		Cohesive	Adhesive	Combined
Without thermocycling treatment	59.7 (4.3) *	2	1	5
VITALi850D with thermocycling 5,000 cycles	39.6 (9.7)	—	—	8
VITALi850D with thermocycling 10,000 cycles	37.0 (8.8)	—	—	8

(* indicates statistically significant difference at $p<0.05$, Ψ indicates number of specimens)

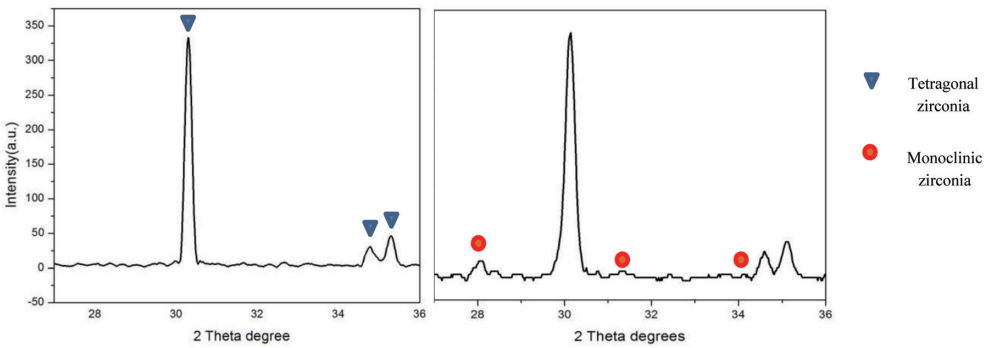

Fig. 5 Representative XRD patterns of VITALi850 before thermocycling (a) and after thermocycling at 5,000 cycles (b).

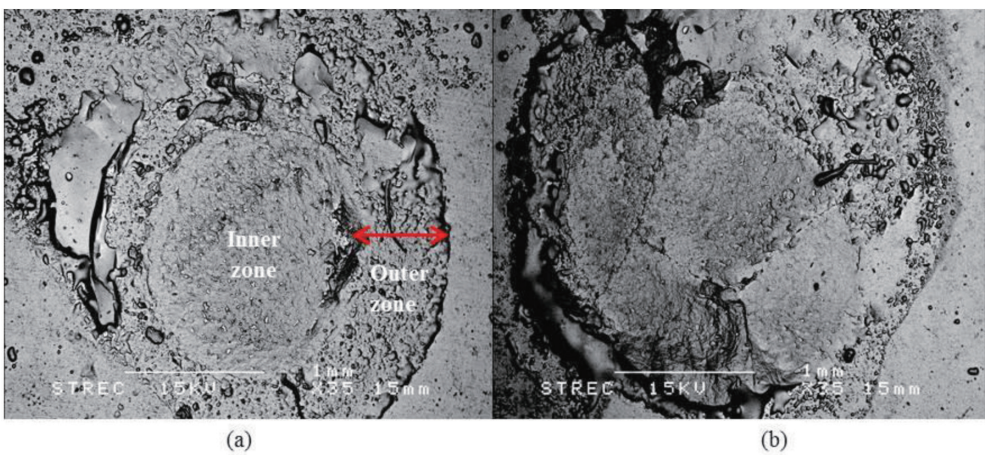

Fig. 6 Back-scattered SEM images of the zirconia surface of fractured VITALi850 specimens: (a) An outer corroded zone and an inner intact zone after 5,000 thermocycles; (b) A completely corroded surface after 10,000 thermocycles.

glass-ceramic liner present on the zirconia surfaces of VITALi850 specimens. Surface of the specimen that was thermocycled 5,000 times revealed an outer zone of corrosion with pits and fissures and an inner non-corroded zone (Fig. 6a). In contrast, the specimen that was thermocycled 10,000 times was corroded across its entire surface (Fig. 6b).

DISCUSSION

Shear bond strength measurements showed that veneering porcelain on zirconia with lithium disilicate glass-ceramic liner fired at 850ºC (VITALi850) had the highest mean SBS. This favorable SBS result could be attributed to the difference in the mineral phase composition of glass-ceramic liner. Unlike the glass matrix, the contents of lithium orthophosphate and lithium disilicate crystals (flexural strength is 350–450 MPa[15]) which contribute to high strength, decrease with increasing firing temperature. This also explained the lower SBS of VITALi900 group.

However, the glass matrix is needed in the wetting of zirconia substructure surface to ensure good diffusion bonding. Therefore, the absence of glass matrix formation at a low firing temperature led to the low mean SBS of VITALi800 group.

It has been reported that the probable cause of porcelain chipping leading to delamination is due to the stress generated by CTE mismatch between the zirconia substructure and veneering porcelain[16,17]. In the case of lithium disilicate, CTE mismatch would be less of a consequence since it has a low CTE[12], which is also compatible with both feldspathic porcelain and zirconia. Therefore, the CTE of lithium disilicate glass-ceramic liner tends to be stable after multiple firings.

The morphology of each crystal phase of glass-ceramic after heat treatment may have an effect on bond strength. Through the preliminary analysis, the microstructures of lithium disilicate glass-ceramic fired at different temperatures demonstrated the influence of time and temperature on microstructural evolution. For VITALi800 and VITALi900, proper melting did not occur: there were void spaces around the glass-ceramic particles when fired at a low temperature or

the formation of a homogeneous glassy matrix at high temperature. Long needle-like $Li_2Si_2O_5$ crystals were observed at 850°C. Such a crystal morphology could have a higher potential to withstand applied forces and resist crack propagation[18].

The firing schedule of veneering porcelains involves multiple firings designed to retain the microstructure of the porcelain and shape of the veneer. Thus, the firings are done at high firing and cooling rates but of short duration. These are done to achieve good diffusion bonding between the adjacent veneering layers.

In this study, after firing the first layer of glass-ceramic liner at 850°C, the microstructure presented many large pores in close proximity. The base layer of dentin porcelain fired at 930°C could then easily penetrate the pores and fuse with lithium disilicate glass-ceramic, forming a strong glassy diffusion bond. As the glass-ceramic liner progressively melted, the fluid glassy matrix with small needle-like shaped crystals could further flow into the surface irregularities of the zirconia substructure, forming a strong micromechanical bond.

When the primary and secondary dentin porcelain layers were fired at temperatures of 910°C and 900°C respectively, diffusion bonding was created between the primary and secondary porcelain layers. This enhanced the overall cohesion for the veneer. Therefore, the highest shear bond strength of VITALi850 was a result of lithium disilicate glass-ceramic forming good adhesion to zirconia and the two veneering porcelain layers. Moreover, the increased mechanical strength of VITALi850 could have resulted in the combined failure mode observed in lithium disilicate glass-ceramic liner, as shown in the back-scattered SEM image (Fig. 4).

After thermocycling, the mean SBS of porcelain-veneered zirconia with lithium disilicate glass-ceramic liner was dramatically decreased. Based on our experimental observation, it was probable that hydrolysis weakened the bond between the glass-ceramic interlayer and zirconia by dissolution. Both ions and crystals were released from the glass-ceramic into the solution, consequently exposing the zirconia interface to hydrolysis as well. Glass corrosion (at pH 2, 7 and 10) caused by hydrolysis had been reported by Esquivel-Upshaw *et al.*[19]. They showed that leaching of ions could occur in neutral as well as in acidic and alkaline environments[19]. In the present study, the effect of leached ions was not investigated.

Even when thermocycled at low temperature, hydrolysis and stress generated by thermal shock might induce the transformation of zirconia from the metastable tetragonal phase to the stable monoclinic phase (Fig. 5) with 4.5 v% expansion[20,21]. Stress accumulated in the zirconia surface after thermocycling was released during the SBS test, thus resulting in crack propagation across the entire interface of VITALi850 specimens after 10,000 times of thermocycling.

The release of accumulated stress during porcelain firing should not be overlooked. Promising findings of the present study warrant future clinical study in search of a better solution to reduce porcelain chipping/delamination from zirconia substructures.

However, results of the present study did not agree with a previous research which found that shear bond strength between zirconia substructure and veneering porcelain was not affected by thermocycling[22]. The contradiction could stem from the great difference in bonding area size, which was three times greater than that of the present study.

CONCLUSIONS

Mean SBS between veneering porcelain and zirconia substructure was significantly improved with lithium disilicate glass-ceramic liner. Within the limitations of this study, factors that led to the improved SBS are given as follows:

1. Firing temperature had an effect on the contents of crystal phases and microstructure of lithium disilicate glass-ceramic liner. Notably, the firing temperature of glass-ceramic liner (first layer) had an effect on the SBS between zirconia and veneering porcelain.
2. Optimal contents of glass matrix and crystal phases with high strength were needed to form strong diffusion bonding between glass-ceramic liner and zirconia substructure.
3. Good cohesion between glass-ceramic liner and veneering porcelain.

ACKNOWLEDGMENTS

This work was supported by the Office of The Higher Education Commission, Ministry of Education of Thailand, under the Project "Strategic Scholarships for Frontier Research Network".

We thank Dr. Kevin Tompkins, Faculty of Dentistry, Chulalongkorn University, and Prof. Serena Best, Director of Cambridge Center for Medical Materials, Department of Materials Science and Metallurgy, University of Cambridge, UK, for critical review of this manuscript.

REFERENCES

1) Koenig V, Vanheusden AJ, Le Goff SO, Mainjot AK. Clinical risk factors related to failures with zirconia-based restorations: An up to 9-year retrospective study. J Dent 2013; 41: 1164-1174.
2) Liu Y, Liu G, Wang Y, Shen JZ, Feng H. Failure modes and fracture origins of porcelain veneers on bilayer dental crowns. Int J Prosthodont 2014; 27: 147-150.
3) Monaco C, Caldari M, Scotti R. Clinical evaluation of 1,132 zirconia-base single crowns: a retrospective cohort study from the AIOP clinical research group. Int J Prosthodont 2013; 26: 435-442.
4) Kim HJ, Lim HP, Park YJ, Vang MS. Effect of zirconia surface treatments on the shear bond strength of veneering ceramic. J Prosthet Dent 2011; 105: 315-322.
5) Kim ST, Cho HJ, Lee YK, Choi SH, Moon HS. Bond strength of Y-TZP–zirconia ceramics subjected to various surface roughening methods and layering porcelain. Surf Int Anal

2010; 42: 576-580.
6) Saied MA, Lloyd IK, Haller WK, Lawn BR. Joining dental ceramic layers with glass. Dent Mater 2011; 27: 1011-1016.
7) Yi Z, Chi Q, Jianqing W, LU Ming L, Pinggen R, Xiaoxi L. Synthesis of leucite from potash feldspar. Journal of Wuhan University of Technology Mater Sci Ed 2008; 23: 452-455.
8) Denry IL. Chapter 11: Restorative materials —Ceramics. In: Sakaguchi RL and Powers JM, editors. Craig's restorative dental materials. 13th ed. St. Louis: Mosby; 2012. pp. 253-276.
9) Mackert JR Jr, Twiggs SW, Williams AL. High-temperature X-ray diffraction measurement of sanidine thermal expansion. J Dent Res 2000; 79: 1590-1595.
10) Mrazova M, Klouzkova A. Leucite porcelain fused to metals for dental restoration. Ceramics-Silikáty 2009; 53: 225-230.
11) Piche PW, O'Brien WJ, Groh CL, Boenke KM. Leucite content of selected dental porcelains. J Biomed Mater Res 1994; 28: 603-609.
12) El-Meliegy E, Noort RV. Glasses and glass ceramic for medical applications. London: Springer Science+Business Media; 2012. pp. 209-228.
13) Monmaturapoj N, Lawita P, Thepsuwan W. Characterisation and properties of lithium disilicate glass ceramics in the SiO2-Li2O-K2O-Al2O3 system for dental applications. Adv Mater Sci Eng 2013; 2013: 1-11.
14) ISO/TS 11405:2003. Dental materials —Testing of adhesion to tooth structure. International Organization for Standardization, Geneva, 2003.
15) Shenoy A, Shenoy N. Dental ceramics: An update. J Conserv Dent 2010; 13: 195-203.
16) Guazzato M, Proos K, Quach L, Swain MV. Strength, reliability and mode of fracture of bilayered porcelain/zirconia (Y-TZP) dental ceramics. Biomaterials 2004; 25: 5045-5052.
17) Thompson JY, Stoner BR, Piascik JR, Smith R. Adhesion/cementation to zirconia and other non-silicate ceramics: Where are we now? Dent Mater 2011; 27: 71-82.
18) Belyakov AV, Bakunov VS. Development of rugged and crack-resistant structures in ceramics (review). Glass and Ceram 1998; 55: 13-18.
19) Esquivel-Upshaw JF, Dieng FY, Clark AE, Neal D, Anusavice KJ. Surface degradation of dental ceramics as a function of environmental ph. J Dent Res 2013; 92: 467-471.
20) Hjerppe J, Vallittu PK, Fröberg K, Lassila LVJ. Effect of sintering time on biaxial strength of zirconium dioxide. Dent Mater 2009; 25: 166-171.
21) Kelly JR, Denry IL. Stabilized zirconia as a structural ceramic: An overview. Dent Mater 2008; 24: 289-298.
22) Guess PC, Kulis A, Witkowski S, Wolkewitzb M, Zhang Y, Strub JR. Shear bond strengths between different zirconia cores and veneering ceramics and their susceptibility to thermocycling. Dent Mater 2008; 24: 1556-1567.